American Mineralogist, Volume 84, pages 384–388, 1999

Elastic wave velocities of $Mg_3Al_2Si_3O_{12}$-pyrope garnet to 10 GPa

Ganglin Chen,[1,*] Joseph A. Cooke Jr.,[2] Gabriel D. Gwanmesia,[1,3] and Robert C. Liebermann[2,†]

[1]Center for High Pressure Research, and Mineral Physics Institute,
State University of New York at Stony Brook, Stony Brook, New York 11794-2100, U.S.A.
[2]Center for High-Pressure Research, and Department of Geosciences,
State University of New York at Stony Brook, Stony Brook, New York 11794-2100, U.S.A.
[3]Department of Physics and Pre-Engineering, Delaware State University, Dover, Delaware 19901, U.S.A.

Abstract

Elastic wave velocities of $Mg_3Al_2Si_3O_{12}$ pyrope garnet were measured to 10 GPa at ambient temperature, using ultrasonic interferometry in a 1000 ton split-cylinder, multi-anvil apparatus (USCA-1000). The sample used in the ultrasonic measurements was a polycrystalline specimen hot-pressed at 5 GPa and 1350 °C in a 2000 ton uniaxial split-sphere apparatus (USSA-2000) from a homogeneous glass of pyrope composition. Special *P-T* paths used during synthesis minimized effects of decompressing and thermal cracking; the bulk density of the sample was indistinguishable from the X-ray density. The elastic wave velocities measured at the ambient condition agree with the Hashin-Shtrikman averages of the single crystal values within the mutual uncertainties. The high-pressure experiments yielded the elastic moduli and their pressure derivatives (finite strain fit) for the shear modulus $G_0 = 92 \pm 1$ GPa, $G_0' = (\partial G/\partial P)_T = 1.6 \pm 0.2$ and for the longitudinal modulus $L_0 = 294 \pm 1$ GPa, $L_0' = (\partial L/\partial P)_T = 7.4 \pm 0.5$, ($L = K_S + 4/3G$), from which the bulk modulus $K_0 = 171 \pm 2$ GPa, $K_0' = (\partial K_S/\partial P)_T = 5.3 \pm 0.4$ was calculated. The pressure derivative for the shear modulus of pyrope did not differ from those of natural pyrope-almandine-grossular garnets. For the bulk modulus, the pressure derivative for pyrope agreed with that for pyrope-almandine but was substantially higher (25%) than that for the Ca-bearing garnet. In the pyrope-majorite series, K_0' remained constant, whereas G_0' increased by 25 for 38% majorite content.

Introduction

High-pressure petrological studies indicate that garnets are prominent mineral constituents in the transition zone of the Earth's mantle (depths of 400 to 700 km) for a wide variety of chemical compositional models; the volume fraction of garnets in this region ranges from ~40% for pyrolite to more than 70% for C1 carbonaceous chondritic compositions (e.g., Ita and Stixrude 1992). The composition of these transition zone garnets lies primarily along the enstatite-pyrope join (Irifune and Ringwood 1987), with the entatite end-member being $MgSiO_3$-majorite. Therefore, knowledge of the elasticity of pyrope-majorite (Py-Mj) garnets is critical in interpreting seismic models of the elastic wave velocities and densities in the transition zone.

Despite a wealth of elasticity data for natural aluminous garnets in the pyrope-almandine-grossular series, until recently very few data have been available for the more Si-rich garnets along the Py-Mj join. Static compression studies of the pressure-volume behavior (e.g., Hazen et al. 1994) have yielded information on the isothermal bulk modulus (K_T) and its pressure derivative (K_{T0}') but none on the shear modulus; furthermore, fitting such *P-V* data to an equation of state has required a significant tradeoff between the bulk modulus and its pressure derivative (e.g., Yagi et al. 1992; Wang et al. 1997).

Studies of the elasticity of Py-Mj garnets at ambient conditions have been performed by Brillouin spectroscopy (e.g., Leitner et al. 1980; Bass and Kanzaki 1990; Yeganeh-Haeri et al. 1990; O'Neill et al. 1991; Pacalo and Weidner 1997; Sinogeikin et al. 1997). High-pressure work above 1 GPa has been limited to studies of natural garnets using both ultrasonic (Webb 1989) and impulsive stimulated scattering (Chai et al. 1997) techniques, with the exception of the work of Rigden et al. (1994) on a synthetic $Py_{62}Mj_{38}$ specimen.

Using techniques developed recently in the authors' multi-anvil, high-pressure laboratory for hot-pressing polycrystalline aggregates of high-pressure phases (Gwanmesia et al. 1993) and for measuring their elastic properties to 10 GPa by ultrasonic techniques (Li et al. 1996), a project has been undertaken to synthesize a suite of samples across the Py-Mj join and to characterize their elastic behavior as a function of pressure to conditions

* Present Address: ST541, Exxon Production Research Co., P.O. Box 2189, Houston, Texas 77252-2189, U.S.A.
† E-mail: Robert.Liebermann@sunytsb.edu

0003–004X/99/0003–0384$05.00

approaching those of the transition zone (Gwanmesia et al. 1998; Liu et al. 1998). This paper reports new sound velocity data for the pyrope end-member of this garnet join to 10 GPa at room temperature and compares these data with previous studies at ambient conditions, as well as those at high pressures (see additional details in Cooke 1997; Cooke et al. 1997). Similar studies using Brillouin spectroscopy and single crystals are underway in the laboratories of the Geophysical Laboratory and the University of Illinois (Conrad et al. 1997; Sinogeikin et al. 1998).

Sample synthesis and characterization

The starting material was a homogeneous glass of pyrope ($Mg_3Al_2Si_3O_{12}$) composition prepared by S. Kesson and S.M. Rigden at the Australian National University. The crushed glass was densely packed into platinum capsules, pressure-sealed at room temperature, and inserted in a 14/7.5 mm cell assembly of a 2000 ton uniaxial, split-sphere apparatus (USSA-2000; Liebermann and Wang 1992). A polycrystalline sample was synthesized in run no. 1924 at conditions of 5 GPa and 1350 °C for 2 h using techniques developed by Gwanmesia et al. (1993) and used previously to hot-press the sample for the Rigden et al. (1994) study. An X-ray diffraction spectrum obtained from the end of the cylindrical sample with a Scintag Diffractometer at 1575 watts (45 kV and 35 mA) using a copper $K\alpha$ target agreed closely with the standard pyrope pattern in the JCPDS file (no. 150742). Complete transformation from the starting glass to crystalline pyrope was inferred from the X-ray diffraction spectrum in which no broad glass background was observed (Cooke 1997). The density of the sample, measured with the immersion technique, was 3.57 + 0.03 g/cm^3, within 0.1% of the X-ray density of 3.565 g/cm^3 (Armbruster et al. 1992), thus demonstrating the low porosity of the sample. Chemical analysis of the hot-pressed sample using a Cameca MBX microprobe agreed with the ideal pyrope composition within 0.5% for all elements and with that of the starting glass material.

In preparation for the ultrasonic measurements, the ends of the cylindrical sample (no. 1924) were polished flat and parallel (as checked with optical methods) successively using 9, 6, 3, and 1 μm diamond polishing compounds. The final sample was a disk of length 0.943(2) mm and a diameter of about 3 mm with grain size less than 1 μm.

Ultrasonic measurements

Ultrasonic travel time measurements at 1 atm were performed on the sample with the ANU (Australian National University) ultrasonic interferometer (Niesler and Jackson 1989) using 40 MHz $LiNbO_3$ (41° X-cut for *P* waves and 36° Y-cut for *S* waves) piezoelectric acoustic transducers. For the bench-top measurements, glass acoustic buffer rods were used. The sample was bonded to the buffer rod (with Nonaq stopcock grease for *P* waves and Dow-Corning resin 276-V9 for *S* waves) and the acoustic echoes from the buffer rod-sample interface and from the free end of the sample were overlapped and interfered. Travel times of the sample were calculated from the interference pattern with an accuracy of 0.5% after correction for the bond effects. The high-pressure ultrasonic experiments were performed in a uniaxial split-cylinder, high-pressure apparatus (USCA-1000) with a force capacity of 1000 tons (5 MN) using ultrasonic interferometric techniques developed in the authors' laboratory for multi-anvil apparatus (Li et al. 1996). The sample was surrounded by lead, housed in a pyrophyllite octahedron, and compressed in the cavity formed by eight truncated tungsten carbide cubes. One of the tungsten carbide cubes also functioned as the acoustic buffer rod with the $LiNbO_3$ transducer mounted on a stress-free truncated corner. A bismuth wire was embedded in a teflon disk directly next to the sample in each run, providing the in-situ pressure marker (from phase transitions at 2.5 and 7.7 GPa) for the ultrasonic experiments.

Results and discussion

Ultrasonic measurements of the *P*- and *S*-wave velocities and the elastic moduli for the polycrystalline pyrope sample at ambient conditions (Table 1) agreed within the mutual uncertainties with those calculated from the single crystal elastic moduli of Leitner et al. (1980) and O'Neill et al. (1991), using the Hashin-Shtrikman averaging scheme. This confirmed the high acoustic quality of this polycrystalline sample and was consistent with its low porosity. Also listed in Table 1 are the sound velocities and moduli for two natural garnets, a pyrope-almandine (Webb 1989) and a pyrope-almandine-grossular (Chai et al. 1997) for which pressure derivatives are also available, as well as those for synthetic grossular (Bass 1989) and pyrope-majorite (Rigden et al. 1994) garnets. These data showed that Fe (almandine) substitution for Mg (pyrope) did not significantly affect either *K* or *G*, confirming an earlier conclusion of Leitner et al. (1980); this is in marked contract with the strong dependence of *G* on Fe content in olivines, orthopyroxenes, and magnesiowüsites (Jackson et al. 1978). The effect of the Ca content is ambiguous: the pure grossular data (Bass 1989) suggests that Ca decreased K by 2% while increasing G by 17%, relative to pyrope; however, these effects were much less pronounced when using the $Py_{52}Al_{32}Gr_{16}$ data of Chai et al. (1997).

The travel times of both *P* and *S* waves were measured to 10 GPa at room temperature using the phase comparison interferometric technique and frequencies between 30 and 60 MHz. The acoustic echo patterns remained excellent to the highest pressures achieved (Fig. 1). The travel time vs. pressure data (Table 2) were corrected for sample length change using the self-consistent method of Cook (1957), as well as the thermal expansivity data of Anderson and Isaak (1995) to convert from the adiabatic to the isothermal bulk modulus. From these corrected travel times, velocities and elastic moduli are tabulated in

TABLE 1. Elasticity of pyrope-rich garnets

	Ambient properties								
Composition	Density g/cm³	v_p km/s	v_s km/s	K_0 GPa	G_0 GPa	L_0 GPa	K_0'	G_0'	L_0'
Py_{100} S*	3.57(2)	9.07(5)	5.07(3)	171(2)	92(1)	294(1)	5.3(4)	1.6(2)	7.4(5)
Py_{100} S†	3.56	9.11	5.02	176	89	295	—	—	—
Py_{100} N‡	3.57	9.10	5.08	173	92	296	—	—	—
$Py_{62}Al_{36}Gr_2$N§	3.84	8.84	4.97	174	95	300	4.9(1)	1.6(1)	7.0(2)
$Py_{52}Al_{32}Gr_{16}$N‖	3.81	8.84	5.0	171	95	298	4.1	1.8	6.4
Gr_{100}N#	3.59	9.34	5.50	168	109	313	—	—	—
$Py_{62}Mj_{38}$S**	3.55	9.00(1)	5.19(1)	169(1)	89(1)	288(2)	5.3(2)	2.0(1)	8.0(3)

Notes: Symbols are as follows: v_p = compressional wave velocity, v_s = shear wave velocity, N = Natural Sample, S = Synthetic Sample, Py = Pyrope $Mg_3Al_2Si_3O_{12}$, Al = Almandine $Fe_3Al_2Si_3O_{12}$, Gr = Grossular $Ca_3Al_2Si_3O_{12}$, Mj = Majorite $Mg_3(MgSi)_2Si_3O_{12}$.

* This Study.
† Leitner et al. (1980).
‡ O'Neill et al. (1991).
§ Webb (1998).
‖ Chai et al. (1997).
Bass (1989).
** Rigden et al. (1994).

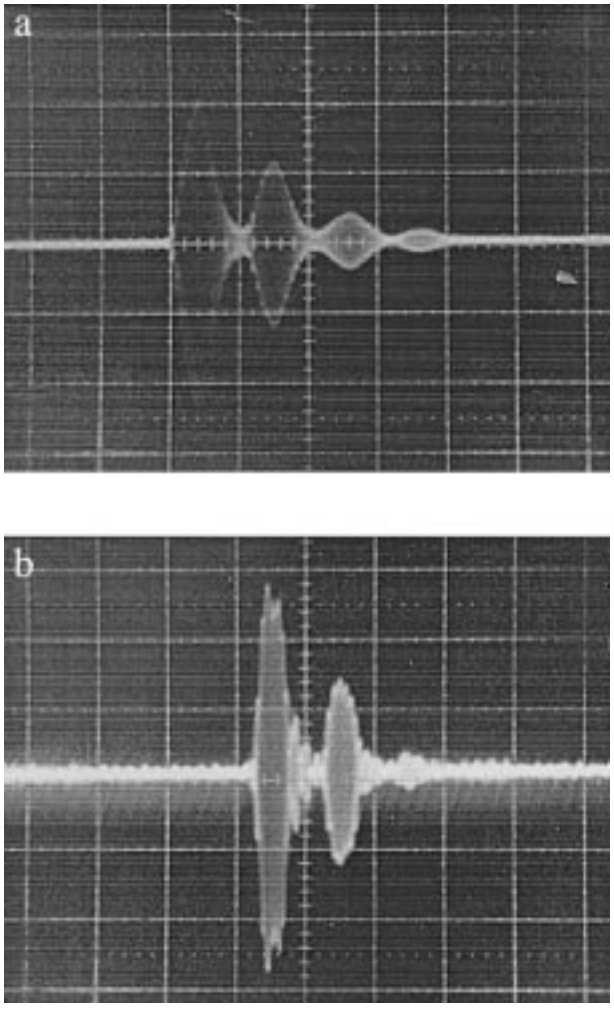

FIGURE 1. Acoustic echo patterns for compressional (*P*) waves in pyrope at ambient conditions (**a**) and at 9.7 GPa (**b**). Successive echoes are from the tungsten carbide buffer rod and round-trip transits in the sample.

Table 2 and plotted in Figures 2 and 3; uncertainties for the velocities were 0.5% and for the moduli 1%.

The measured data for the longitudinal ($K + 4/3G$) and shear moduli were fit with a third-order, Eulerian finite-strain equation of state (e.g., Davies and Dziewonski 1975) to obtain the values of the moduli at zero pressure (L_0, G_0) and their pressure derivatives (L_0' and G_0'), yielding values of $L_0 = 294 \pm 1$ GPa, $L_0' = (\partial L/\partial P)_T = 7.4 +$

TABLE 2. Acoustic data for pyrope as a function of pressure at room temperature

Pressure GPa	Travel Time μs	Length mm	v_p km/s	Modulus GPa
		P-wave data		
0.0	0.208	0.943	9.07	294
1.0	0.206	0.941	9.14	300
1.8	0.204	0.940	9.21	306
2.1	0.203	0.939	9.25	309
2.7	0.201	0.938	9.34	316
3.2	0.200	0.937	9.37	319
3.5	0.199	0.937	9.42	323
4.5	0.197	0.935	9.50	330
5.5	0.195	0.934	9.58	337
6.4	0.193	0.932	9.66	345
7.9	0.191	0.930	9.74	353
8.8	0.190	0.929	9.78	357
9.3	0.190	0.928	9.77	358
9.7	0.189	0.927	9.81	362
		S-wave data		
0.0	0.372	0.943	5.07	92
2.4	0.364	0.939	5.16	96
3.2	0.362	0.937	5.18	98
4.1	0.360	0.936	5.20	99
4.9	0.358	0.935	5.22	100
5.7	0.355	0.933	5.26	102
6.5	0.354	0.932	5.27	103
7.3	0.352	0.931	5.29	104
8.2	0.351	0.930	5.30	105
9.0	0.350	0.928	5.31	105

Notes: For the *P*-waves, the modulus is *L,* longitudinal. For the *S*-waves, the modulus is *G,* shear. Uncertainties in the data are travel time = 0.5%; velocity = 0.5%; elastic modulus = 1%. Densities at high pressure were calculated directly from ambient density of 3.57 g/cm³ and length changes derived from acoustic data via Cook's (1957) method.

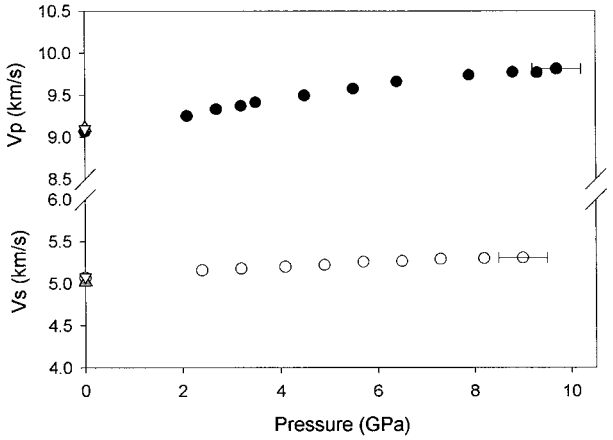

FIGURE 2. *P* and *S*-wave velocities for pyrope garnet as a function of pressure. Error bars are indicated on the last data point. Downward-pointing and upward-pointing triangles at $P = 0$ are for the Hashin-Shtrikman averages of the single crystal moduli from the studies of Leitner et al. (1980) and of O'Neill et al. (1991), respectively.

0.5 and $G_0 = 92 \pm 1$ GPa, $G_0' = (\partial G/\partial P)_T = 1.6 + 0.2$, from which was calculated $K_0 = 171 \pm 2$ GPa, $K_0' = (\partial K_S/\partial P)_T = 5.3 + 0.4$ (Table 1). Also listed are pressure derivatives of the bulk and shear moduli for the natural garnets measured by Webb (1989) and Chai et al. (1997) and the synthetic $Py_{62}Mj_{38}$ garnet of Rigden et al. (1994). The pressure derivative of the shear modulus varied little among the natural garnet compositions. However, for the bulk modulus, substitution of 16 mol% grossular decreases K_0' by 24%; the data for the Py-Al garnet of Webb (1989) agreed with the current values for pyrope within the mutual uncertainties. In the pyrope-majorite series, K_0' was unchanged by the addition of 38 mole% majorite to pyrope, while G_0' increased by 25%. Such high values for the pressure derivatives of the elastic moduli of majorite-rich garnets may be important in explaining the high velocity gradients with depth observed in seismic models of the Earth's transition zone (following Rigden et al. 1994).

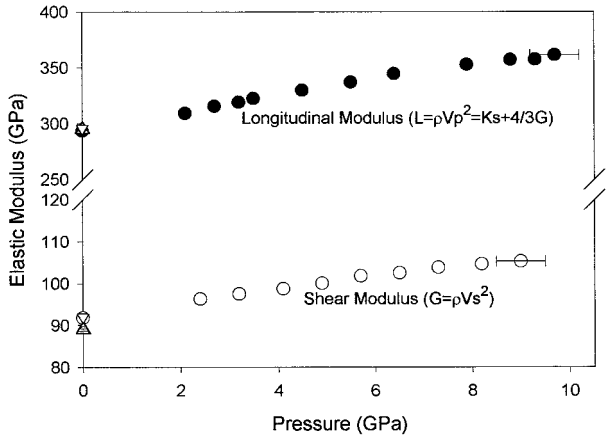

FIGURE 3. Longitudinal and shear moduli for pyrope garnet as a function of pressure. Error bars are indicated in the last data point. Symbols are as in Figure 2.

The results of this study on pyrope garnet, together with companion studies for pyrope-majorite garnets by Liu et al. (1998 for a $Py_{62}Mj_{38}$) and Gwanmesia et al. (1998 for Mj_{100}), provide a compatible data set for constructing a more comprehensive mineralogical model for the transition zone of the Earth mantle.

ACKNOWLEDGMENTS

It is a pleasure to contribute this paper to the Special Issue in honor of Charles T. Prewitt, who was a co-founder of the Stony Brook High Pressure Laboratory in 1985 with R.C. Liebermann and D.J. Weidner. We thank S. Kesson and S.M Rigden for preparation of the starting material, Y.D. Sinelnikov for the microprobe analyses, and Jun Liu for discussions of these experiments. These high-pressure experiments were performed in the Stony Brook High Pressure Laboratory, which is jointly supported by the State University of New York at Stony Brook and the NSF Science and Technology Center for High Pressure Research (EAR 89-20239). This research was also supported by research grants to R.C. Liebermann (EAR 93-04502 and 96-14612). This is MPI contribution No. 243.

REFERENCES CITED

Anderson, O.L. and Isaak, D.G. (1995) Elastic constants of mantle minerals at high temprerature. In T. J. Ahrens, Ed., Mineral Physics and Crystallography: A Handbook of Physical Constants, American Geophysical Union, Washington, D.C.

Armbruster, T., Geiger, C.A., and Lager, G.A. (1992) Single-crystal X-ray structure study of synthetic pyrope almandine garnets at 100 and 293 K. American Mineralogist, 77, 512–521.

Bass, J.D. (1989) Elasticity of grossular and spessartite garnets by Brillouin spectroscopy, Journal of Geophysical Research, 94, 7621–7628.

Bass, J.D. and Kanzaki, M., (1990) Elasticity of a majorite-pyrope solid solution. Geophysics Research Letters, 17, 1989–1990.

Chai, M., Brown, J.M., and Slutsky, L.J. (1997) The elastic constants of a pyrope-grossula-almandine garnet to 20 GPa. Geophysical Research Letters, 24, 523–526.

Conrad, P.G., Zha, C-S., Yang, H., Mao, H-K., and Hemley, R.J. (1997) Measurement of pyrope elasticity by Brillouin scattering at high pressures. Eos, 78, 5312.

Cook, R.K. (1957) Variation of elastic constants and static strains with hydrostatic pressure: a method for calculation from ultrasonic measurements. Journal of the Acoustical Society of America, 29, 445–449.

Cooke, J.A. Jr., (1997) Ultrasonic measurements of the elastic wave velocities of $Mg_3Si_3O_{12}$ pyrope-garnet to 9 GPa at room temperature. Master's Thesis, State University of New York at Stony Brook, Stony Brook, N.Y.

Cooke, J.A. Jr., Chen, G., Gwanmesia, G.D., and Liebermann, R.C. (1997) Elastic wave velocities of pyrope garnet $Mg_3Al_2Si_3O_{12}$ to 9 GPa at room temperature, EOS, 78, S312.

Davies, G.F. and Dziewonski, A.M. (1975) Homogeneity and constitution of the Earth's lower mantle and outer core. Physics of the Earth and Planetary Interiors, 10, 336–343.

Gwanmesia, G.D., Li, B., and Liebermann, R.C. (1993) Hot pressing of polycrystals of high-pressure phases of mantle minerals in multi-anvil apparatus. Pure and Applied Geophysics, 141, 467–484.

Gwanmesia, G.D., Chen, G, Liu, J. and Liebermann, R.C. (1998) Elasticity of polycrystalline $MgSiO_3$-garnet to 8 GPa at room temperature. EOS, 79, S163.

Hazen, R.M., Downs, R.T., Conrad, P.G., Finger, L.W., and Gasparik, T. (1994) Comparative compressibilities of majorite-type garnets. Physics and Chemistry of Minerals, 21, 344–349.

Irifune, T. and Ringwood, A.E. (1987) Phase transformations in primative MORB and pyrolite compositions to 25 GPa and some geophysical implications. In M. H. Manghnani and Y. Syono, Eds., High-Pressure

Research in Geophysics, p. 231–242. American Geophysical Union, Washington, D. C.

Ita, J. and Stixrude, L. (1992) Petrology, elasticity, and composition of the mantle transition zone. Geophysical Research Letters, 97, 6849–6866.

Jackson, I., Liebermann, R.C., and Ringwood, A.E. (1978) The elastic properties of (Mg,Fe) solid solutions. Physics and Chemistry of Minerals, 3, 1–31.

Leitner, B.J., Weidner, D.J., and Liebermann, R.C. (1980) Elasticity of single crystal pyrope and implications for garnet solid solution series. Physics of the Earth and Planetary Interiors, 22, 111–121.

Li, B., Jackson, I., Gasparik, T., and Liebermann, R.C. (1996) Elasticity wave velocity measurement in multi-anvil apparatus to 10 GPa using ultrasonic interferometry. Physics of the Earth and Planetary Interiors, 98, 79–91.

Liebermann, R.C. and Wang, Y. (1992) Characterization of sample environment in multi-anvil split-sphere apparatus. In Y. Syono and M. H. Manghnani, Eds., High-Pressure Research: Application to Earth and Planetary Sciences. Geophysics Monograph Series, 67, Terra Publications, Tokyo-American Geophysical Union, Washington, D.C.

Liu, J., Chen, G., Gwanmesia, G.D., and Liebermann, R.C. (1998) Elasticity of pyrope-majorite garnet to 8 GPa. EOS, 79, S162.

Niesler, H. and Jackson, I. (1989) Pressure derivatives of elastic wave velocities from ultrasonic interometric measurements on jacketed polycrystals. Journal of Acoustical Society of America, 86, 1573–1585.

Pacalo, R.E.G. and Weidner, D.J. (1997) Elasticity of majorite, $MgSiO_3$ tetragonal garnet. Physics of the Earth and Planetary Interiors, 99, 145–154.

O'Neill, B., Bass, J.D., Rossman, G.R., Geiger, C.A., and Langer, K. (1991) Elastic properties of pyrope. Physics and Chemistry of Minerals, 77, 617–621.

Rigden, S.M., Gwanmesia, G.D., and Liebermann, R.C. (1994) Elastic wave velocities of a pyrope-majorite garnet to 3 GPa. Physics of the Earth and Planetary Interiors, 86, 35–44.

Sinogeikin, S.V., Bass, J.D., O'Neill, B., and Gasparik, T. (1997) Elasticity of tetragonal end-member majorite and solid solutions in the system $Mg_4Si_4O_{12}$-$Mg_3Al_2Si_3O_{12}$. Physics and Chemistry of Minerals, 24, 115–121.

Sinogeikin, S.V. and Bass, J.D. (1998) Single crystal elasticity of synthetic pyrope and MgO by Brillouin Scattering to 20 GPa. EOS, 79, S163.

Wang, Y., Weidner, D.J., Zhang, J., Gwanmesia, G.D., and Liebermann, R.C. (1997) Thermal equation of state of garnets along the pyrope-majorite join. Physics of the Earth and Planetary Interiors, 105, 59–71.

Webb, S. L. (1989) The elasticity of the upper mantle orthosilicates olivine and garnet to 3 GPa. Physics and Chemistry of Minerals, 16, 684–692.

Yagi, T., Uchiyama, Y., Akaogi, M., and Ito, E. (1992) Isothermal compression curve of $MgSiO_3$ tetragonal garnet. Physics of the Earth and Planetary Interiors, 74, 1–7.

Yeganeh-Haeri, A. and Weidner, D.J. (1990) Elastic properties of the pyrope-majorite solid solution series. Geophysical Research Letters, 17, 2453–2456.

Manuscript received June 29, 1998
Manuscript accepted October 13, 1998
Paper handled by William A. Bassett